

3-5-1990

## Approximate Solutions of the Boltzmann Equation for Secondary Electron Emission: Results and Comparisons to Experiments

A. Dubus

*Université Libre de Bruxelles*

J. Devooght

*Université Libre de Bruxelles*

J. C. Dehaes

*Université Libre de Bruxelles*

Follow this and additional works at: <https://digitalcommons.usu.edu/microscopy>



Part of the [Biology Commons](#)

---

### Recommended Citation

Dubus, A.; Devooght, J.; and Dehaes, J. C. (1990) "Approximate Solutions of the Boltzmann Equation for Secondary Electron Emission: Results and Comparisons to Experiments," *Scanning Microscopy*. Vol. 4 : No. 1 , Article 1.

Available at: <https://digitalcommons.usu.edu/microscopy/vol4/iss1/1>

This Article is brought to you for free and open access by the Western Dairy Center at DigitalCommons@USU. It has been accepted for inclusion in Scanning Microscopy by an authorized administrator of DigitalCommons@USU. For more information, please contact [digitalcommons@usu.edu](mailto:digitalcommons@usu.edu).



APPROXIMATE SOLUTIONS OF THE BOLTZMANN EQUATION FOR SECONDARY ELECTRON EMISSION :  
RESULTS AND COMPARISONS TO EXPERIMENTS

A. DUBUS<sup>\*,\*\*</sup>, J. DEVOOGHT and J.C. DEHAES

Université Libre de Bruxelles  
Service de Métrologie Nucléaire (C.P. 165)  
50, av. F.D. Roosevelt  
B-1050 Brussels , Belgium

(Received for publication January 17, 1990, and in revised form March 5, 1990)

Abstract

The aim of the present paper is to survey the theoretical work performed in Brussels about secondary electron emission (SEE). Two new approximate solutions of the Boltzmann equation for internal secondary electrons are applied to both electron and ion induced SEE. Using a realistic set of interaction cross sections, most calculated characteristics of electron emission compare fairly well to experiments.

The "improved age-diffusion" model can be used to calculate the electron yield, the energy and angular spectrum and also the depth and radial distributions of outgoing electrons for incident electrons and ions.

The "transport-albedo" model assumes a uniform internal electron source in a semiinfinite medium and gives the electron yield and the energy spectrum of secondary electrons for incident light ions. Taking into account the anisotropy of the internal electron source, the ratio of the forward and backward yields and the influence of the angle of incidence have been calculated for thin targets.

Key Words: Electron-induced secondary electron emission, ion-induced secondary electron emission, comparisons between incident electrons and ions, transport theory, secondary electron yield, secondary electron energy distribution, depth and radial distributions, time distribution, forward to backward yield ratio, influence of the tilt angle of the target

\* Address for correspondence:  
A. DUBUS , Université Libre de Bruxelles, Service de Métrologie Nucléaire (C.P. 165) - 50 av. F.D. Roosevelt - B-1050 Brussels , BELGIUM,  
Phone No. (32) 2 - 642 20 59

\*\* Chargé de Recherches du Fonds National Belge de la Recherche Scientifique

Introduction

When fast, charged particles penetrate into a solid target, low energy electrons (a few eV) are emitted as a consequence of inelastic interactions of the incident particles with the electrons and atoms of the target. Such electrons are called secondary electrons (SE).

This phenomenon, evidenced in 1902 by Austin and Starke (1902), has been up to now the object of many experimental and theoretical works.

Except for the pioneering work of Bethe (1941), the first theory dealing with both electron and ion induced SEE had been published in 1980 by Schou (1980a,b) (we use SEE for ions instead of ion induced electron emission (IIEE)). Afterwards, a few other theories had been proposed (Rösler and Brauer, 1981a,b, 1984, 1988, Brauer and Rösler, 1985, Devooght et al., 1984, 1987a,b, Dubus et al., 1986, 1987). Review papers (Sigmund and Tougaard, 1981, Hasselkamp, 1985, Schou, 1988, 1989) discussing and comparing both incident electron and ion induced emissions have been published.

This paper gives a survey of the two new SEE models developed in Brussels and based upon neutron transport and radiative transfer techniques: the "improved age-diffusion" model (Devooght et al., 1987b, Dubus et al., 1987) and the "transport-albedo" model (Devooght et al., 1987a) and their application to both electron and ion induced SEE is reviewed.

Theoretical Description of SEE

The first simple transport models of SEE from a semiinfinite solid target are given by Baroody (1950) and Bruining (1954), among others, for incident electrons (keV range) and by Sternglass (1957) for incident ions (100 keV-1 MeV range). In these models, the successive stages of the emission process are clearly distinguished: the primary particle penetrates into the target, and excites internal SE along its path, the electrons interact with the solid via elastic and inelastic collisions, some electrons arriving at the surface of the solid can escape through the vacuum-solid interface. These models have been improved (for incident electrons) by Wolff (1954) and Stolz (1959) who introduced explicitly the electron cascade in the emission process and gave the first

approximate solution of the Boltzmann transport equation for SEE, i.e., the "infinite medium slowing down" model.

The most recent models of electron emission can be classified in three categories: the first two, i.e., the Monte Carlo calculations and the approximate solutions of the Boltzmann equation, use microscopic interaction cross sections, while the third one, i.e. Schou's model (Schou, 1980a,b) is based on an analogy between SEE and sputtering and uses as input data macroscopic quantities such as the stopping power and the energy deposition law in the target.

Koshikawa and Shimizu (1974) and Ganachaud and Cailler (1979a,b) have developed direct Monte Carlo calculations for electron induced SEE. They used microscopic cross sections for electron interactions in the target. It is worth noting that the description of electron interactions given by Ganachaud and Cailler (1979a) is one of the most elaborate but it is essentially limited to nearly free electron materials such as polycrystalline Al targets (an extension to noble metals can be found in Ganachaud's thesis (1977)).

Bindi et al. (1980a,b,c) and Lanteri et al. (1979,1982) have solved the Boltzmann equation for SE transport by a direct numerical solution ( $S_N$ -multigroup method). They have applied their model to SEE and to electron backscattering and transmission. Recently, Rostaing et al. (1986) and Lanteri et al. (1986) have used the interaction cross sections developed by Ganachaud and Cailler (1979a) and they have calculated the characteristics of electron backscattering and transmission for polycrystalline Al targets.

Rösler and Brauer have developed a realistic set of interaction cross sections for ion and electron interactions in polycrystalline Al targets and have used the "infinite medium slowing down" model for electron transport (Rösler and Brauer, 1981a,b,1984,1988, Brauer and Rösler, 1985).

Bindi et al. (1987) have discussed most of these contributions.

#### Characteristics of our Models

Our electron transport models (Dubus, 1987), i.e., the "improved age-diffusion" model (Devooght et al., 1984,1987b, Dubus et al., 1987) and the "transport-albedo" model (Dubus et al., 1986, Devooght et al., 1987a) are approximate solutions of the Boltzmann equation and hence are comparable to the calculations of Bindi et al. (1980a,b,c), Lanteri et al. (1979,1982) and Rösler and Brauer (1981a,b).

The "improved age-diffusion" model is analytical and can be used for a parametric study of electron emission, i.e., a study of the influence of the choice of a model of cross section, for instance.

The "transport-albedo" model improves the "infinite medium slowing down" model since it takes into account the partial reflection boundary condition. It is as much as possible, analytical in order to reduce the computer time.

These models and the interaction cross sections that we have used in our calculations are briefly described in this paper.

We insist particularly that both electron and ion induced SEE can be calculated in the same way.

Then, we describe our most important results and we give some comparisons between the existing models for electron emission.

#### SE Transport Models

##### Electron and ion induced SEE

Electron induced SEE and light ion ( $H^+$  for instance) induced kinetic SEE are similar phenomena (Sigmund and Tougaard, 1981, Hasselkamp, 1985, Schou, 1988).

In both cases, the emission process can be split into three stages:

- 1) The primary particle penetrates into the target and gives rise to primary ionization, i.e., internal SEE excitation by the primaries.
- 2) The internal secondaries slow down, multiply and may migrate to the surface.
- 3) Some electrons can escape through the vacuum-medium interface which is treated as a potential barrier of height  $U_0$  with specular reflection of the non-escaping electrons.

It is worth noting that stages 2 and 3 are not really separate since some electrons can escape during the slowing down and multiplication process.

In our calculations, the first stage, i.e., the internal electron source, must be calculated separately. Our models consider really the semiinfinite character of the target for the transport of electrons and, as a consequence, stages 2 and 3 are not separate.

Electron induced SE and ion induced SE only differ by the first stage of the emission process.

Recently, Hasselkamp (1985) and Schou (1988) have compared the ionization cross sections for incident electrons and ions. These cross sections are similar when the incident particles have the same velocity  $v$  (Schou,1988).

The most important difference between primary electrons and primary ions resides in their trajectory in the solid.

For  $v \geq 2$  a.u., the backscattering coefficient for light incident ions is much smaller than the backscattering coefficient for incident electrons with the same velocity (Hasselkamp, 1985, Schou, 1988, Bindi et al.,1980c, Tabata et al.,1983, Eckstein and Verbeek,1984). Moreover the energy loss of incident primary electrons in the depth zone from which electrons escape cannot be neglected with respect to their initial energy as is the case for incident light ions.

As has been pointed out by Schou (1988), the ion induced SE yield is equivalent to the partial yield  $\delta_0$  for incident electrons (Seiler,1967, Thomas and Pattinson,1970) and no slow primaries are included in the yield as is the case for the electron induced SE yield.

For incident electrons, we have distinguished primary and secondary electrons. The splitting of electrons in "primaries" and "secondaries" is of course arbitrary since electrons are undistinguishable. However, it appears as a natural consequence of the expression of the interaction cross sections and allows a similar treatment for

electron induced SE and for ion induced SE by the use of an internal SE source. The Boltzmann equation for electron induced SE can be written as:

$$\left[ \frac{1}{v} \frac{\partial}{\partial t} + \vec{\Omega} \cdot \nabla + \Sigma_s(E) \right] \Phi_t(\vec{r}, E, \vec{\Omega}, t) = \int_E^\infty \int_{4\pi} [\Sigma_s(E' \rightarrow E, \vec{\Omega}' \rightarrow \vec{\Omega}) + \Sigma_s^S(E' \rightarrow E, \vec{\Omega}' \rightarrow \vec{\Omega})] \Phi_t(\vec{r}, E', \vec{\Omega}', t) dE' d\vec{\Omega}' \quad (1)$$

$E, v, \vec{\Omega}, \vec{r}$  and  $t$  are the SE energy (in the solid), velocity, direction vector, position and time variable, respectively;  $\Sigma_s(E)$  is the total scattering cross section and  $[\Sigma_s(E' \rightarrow E, \vec{\Omega}' \rightarrow \vec{\Omega}) + \Sigma_s^S(E' \rightarrow E, \vec{\Omega}' \rightarrow \vec{\Omega})]$  is the slowing down kernel.

Equation (1) is a balance equation for the total internal electron flux  $\Phi_t(\vec{r}, E, \vec{\Omega}, t)$  ( $\Phi_t(\vec{r}, E, \vec{\Omega}, t) d\vec{r} dE d\vec{\Omega}$  is the number of electrons in the volume element  $d\vec{r}$  around  $\vec{r}$ , in the energy interval  $(E, E+dE)$  and in the direction (element  $d\vec{\Omega}$  around)  $\vec{\Omega}$  crossing a unit surface orthogonal to  $\vec{\Omega}$  per unit time). In the left-hand side, we have a time dependent term  $\frac{\partial}{\partial t} \Phi_t$ , a spatial dispersion term  $\vec{\Omega} \cdot \nabla \Phi_t$  and an absorption term  $\Sigma_s(E) \Phi_t$ . In the right hand side, we have a slowing down source, i.e., electrons which appear at energy  $E$  coming from energy  $E'$  ( $E' > E$ ). Two slowing down kernels appear in the slowing down source because both the incident and the excited electrons become part of the cascade.  $\Sigma_s(E' \rightarrow E, \vec{\Omega}' \rightarrow \vec{\Omega})$  is the so-called "scattering" cross section and  $\Sigma_s^S(E' \rightarrow E, \vec{\Omega}' \rightarrow \vec{\Omega})$  is the "creation" cross section (see (Devooght et al., 1987b) and below).

The ingoing current and partial reflection boundary condition for one electron of energy  $E_{p0}$ , direction  $\vec{\Omega}_{p0}$  incident at the surface on time  $t_0$  is:

$$\Phi_t(0, \vec{\rho}, E, \vec{\Omega}, t) = \frac{1}{|\mu_{p0}|} \delta(\vec{\Omega} - \vec{\Omega}_{p0}) \delta(E - E_{p0}) \delta(\vec{\rho} - 0) \delta(t - t_0) + H(\mu_c(E) - \mu) \Phi_t(0, \vec{\rho}, E, \vec{\Omega} - 2|\vec{\Omega} \cdot \vec{I}_x| \vec{I}_x, t) \quad (\vec{\Omega} \cdot \vec{I}_x > 0) \quad (2)$$

is the projection of  $\vec{r}$  on the  $x=0$  plane where  $x$  is the depth variable,  $\mu_{p0} = \vec{\Omega}_{p0} \cdot \vec{I}_x$  is the cosine of the penetration angle of the primary electron in the target with respect to the inward normal to the surface  $\vec{I}_x$ .

The first term of the right hand-side of (2) represents the ingoing primary electron flux while the second term represents the partial reflection of electrons at the vacuum-medium interface due to the potential barrier.

The Heaviside step function  $H$  expresses that electrons outside the escape cone ( $\mu < \mu_c(E) = (U_0/E)^{1/2}$ ) are reflected by the barrier and the  $\vec{\Omega} - 2|\vec{\Omega} \cdot \vec{I}_x| \vec{I}_x$  factor expresses the specular reflection

See Symbol Table on pp. 15.

of these electrons.

The geometry of this process is shown in Fig.1.

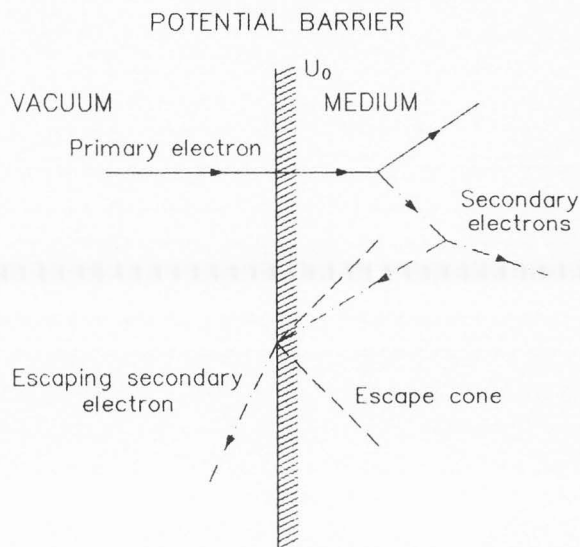


Figure 1. Sketch of the electron induced SE process. The primary electron creates secondary electrons which multiply and can escape through the surface barrier.

The energy and angular dependences of the differential "scattering" and "creation" cross sections are very different ( $E_{p0} \geq 100$  eV) in a nearly free electron material due to the high screening of the electron gas.

Incident electrons are scattered with small energy losses and small angular deflections while the created electrons appear almost isotropically at low energy ( $E \gtrsim E_p$ ).

Due to the specific behaviour of both parts of the slowing down kernel, the total internal electron flux consists approximately of two separate parts: a high energy part ( $E \approx E_{p0}$ ) that can be identified as the primary electrons and a low energy part that can be identified as the true SE. This is evidenced experimentally by the energy spectrum of outgoing electrons (Roepin, 1975).

One can split the internal electron flux in these two components :

$$\Phi_t(\vec{r}, E, \vec{\Omega}, t) = \Phi_p(\vec{r}, E, \vec{\Omega}, t) + \Phi(\vec{r}, E, \vec{\Omega}, t) \quad (3)$$

where  $\Phi_p$  is the primary electron flux and  $\Phi$  is the true SE flux.

The Boltzmann equation for the primary electrons is then :

$$\left[ \frac{1}{v} \frac{\partial}{\partial t} + \vec{\Omega} \cdot \nabla + \Sigma_s(E) \right] \Phi_p(\vec{r}, E, \vec{\Omega}, t) = \int_E^\infty \int_{4\pi} \Sigma_s(E' \rightarrow E, \vec{\Omega}' \rightarrow \vec{\Omega}) \Phi_p(\vec{r}, E', \vec{\Omega}', t) dE' d\vec{\Omega}' \quad (4)$$

and  $\Phi_p$  must satisfy the condition (2).

For the SE, we have

$$\left[ \frac{1}{v} \frac{\partial}{\partial E} + \bar{\Omega} \cdot \bar{\nabla} + \Sigma_s(E) \right] \Phi(\bar{r}, E, \bar{\Omega}, t) = \int \int_{E, 4\pi}^{\infty} [\Sigma_s(E' \rightarrow E, \bar{\Omega}' \rightarrow \bar{\Omega}) + \Sigma_s^5(E' \rightarrow E, \bar{\Omega}' \rightarrow \bar{\Omega})] \Phi(\bar{r}, E', \bar{\Omega}', t) dE' d\bar{\Omega}' + Q(\bar{r}, E, \bar{\Omega}, t) \quad (5)$$

with the boundary condition:

$$\Phi(0, \bar{\rho}, E, \bar{\Omega}, t) = H(\mu_c(E) - \mu) \Phi(0, \bar{\rho}, E, \bar{\Omega} - 2|\bar{\Omega} \cdot \bar{I}_x| \bar{I}_x, t) \quad (6)$$

The internal electron source is given by

$$Q(\bar{r}, E, \bar{\Omega}, t) = \int \int_{E, 4\pi}^{\infty} \Sigma_s^5(E' \rightarrow E, \bar{\Omega}' \rightarrow \bar{\Omega}) \Phi_p(\bar{r}, E', \bar{\Omega}', E) dE' d\bar{\Omega}' \quad (7)$$

For incident ions, no particular problems arise when one calculates the internal electron source. For one ion incident on the surface per unit time and per unit surface, the ion flux  $\Phi_i(\bar{r}, E, \bar{\Omega}, t)$  can be written as :

$$\Phi_i(\bar{r}, E, \bar{\Omega}, t) = \frac{1}{|\mu_i|} \delta(E - E_i) \delta(\bar{\Omega} - \bar{\Omega}_i) \quad (8)$$

where  $E_i$  is the incident ion energy,  $\mu_i = \bar{\Omega}_i \cdot \bar{I}_x$  is the cosine of the incidence angle of the ions. Internal SE are created by ionization and the internal electron source is given by

$$Q(\bar{r}, E, \bar{\Omega}, t) = \int \int_{E_{\min}, 4\pi}^{\infty} \Sigma_i(E' \rightarrow E, \bar{\Omega}' \rightarrow \bar{\Omega}) \Phi_i(\bar{r}, E', \bar{\Omega}', t) dE' d\bar{\Omega}' = \frac{1}{|\mu_i|} \Sigma_i(E_i \rightarrow E, \bar{\Omega}_i \rightarrow \bar{\Omega}) \quad (9)$$

where  $\Sigma_i(E' \rightarrow E, \bar{\Omega}' \rightarrow \bar{\Omega})$  is the differential ionization cross section for incident ions in the target and  $E_{\min}$  the minimum ion energy necessary to create an electron of energy  $E$ .

The stationary ion induced SEE transport equation is equation (5) (without the time derivative term) with the boundary condition (6) and with the internal electron source  $Q$  given by (9).

Electron and ion induced SE are then formally similar. One must solve the Boltzmann equation (5)

with the partial reflection boundary condition (6). The internal electron source for ion induced electron emission (9) is deduced immediately from the ionization cross section while the internal electron source for electron induced electron emission (7) is given as the solution of the primary electron transport equation. It must be pointed out that the internal electron source for fast incident ions is uniform in the SE depth of escape while it is not for incident electrons. We will come back to these problems below.

Improved age-diffusion model (Devooght et al., 1984, 1987b, Dubus et al., 1987)

The "improved age-diffusion" model is analytical insofar as it gives an analytical expression for the outgoing electron flux due to a monoenergetic, monodirectional and instantaneous point source. After the numerical convolution of this Green's function with the internal electron source, one obtains the energy, angle, time and radial distribution of the outgoing electron current at the surface. The medium is homogeneous but the energy, angle, space and time distribution of the internal electron source can be arbitrary. Hence, the "improved age-diffusion" model can be applied to both ion induced SE and electron induced SE. Moreover, the interaction cross sections can be arbitrary, hence realistic.

A last important characteristic of this model is that it keeps the time dependence of electron emission and gives the radial distribution of outgoing electrons. Time dependence is absent from all earlier descriptions of electron emission and has been kept here due to its potential use in beam-foil spectroscopy (Gay and Berry, 1979).

It is evidenced experimentally that the internal electron distribution is nearly isotropic. The Boltzmann equation (5) can then be solved by a classical  $P_1$  approximation (Ferziger and Zweifel, 1966). Introducing a synthetic scattering kernel (Williams, 1966), i.e., a simpler kernel which reproduces the main features of the original kernel, in the  $P_1$  system, one obtains, with the usual assumptions of the diffusion theory (Ferziger and Zweifel, 1966), a diffusion-slowng down equation for the isotropic part of the internal electron flux  $\Phi_0(\bar{r}, E, t)$  :

$$\left[ -D(E) \Delta + \frac{1}{v} \frac{\partial}{\partial E} + \Sigma_0(E) \right] \Phi_0(\bar{r}, E, t) = \int \frac{\Sigma_{rem}(E')}{E' - E_f} \Phi_0(\bar{r}, E', t) dE' + Q_0(\bar{r}, E, t) - 3D(E) \bar{\nabla} \cdot \bar{\Omega}_1(\bar{r}, E, t) \quad (10)$$

$Q_0(\bar{r}, E, t)$  is the isotropic part of the internal electron source and  $\bar{Q}_1(\bar{r}, E, t)$  is the current vector of the internal electron source.

The electron interaction cross sections only appear through the three transport coefficients, i.e.,  $D(E)$ , a diffusion coefficient,  $\Sigma_0(E)$ , an effective absorption cross section and  $\Sigma_{rem}(E)$ , a removal cross section (see Devooght et al., 1987b for further details).

In the diffusion approximation, the boundary condition (6) takes the form of a Neuman-Dirichlet boundary condition (Devooght et al., 1987b).

In order to solve (10), we introduce an approximation similar to the one underlying the Fermi's age theory and obtain an analytical approximation of the Green's function (Devooght et al., 1987b).

The angular distribution of the outgoing electron current is obtained from the expression of the partial reflection boundary conditions in the diffusion approximation (Devooght et al., 1987b).

The input data for the "improved age-diffusion model" are the space, time, energy and angle dependence of the internal electron source and the energy and angular differential cross sections for the electrons in the medium.

Due to its analytical form, this model is well suited to a parametric study of SEE.

The "transport-albedo" model (Devooght et al., 1987a)

The "transport-albedo" model has been designed for uniform internal electron sources. It can be applied to ion induced SEE and high energy ( $E_{\rho 0} > 1$  keV) electron induced SEE (where the source is nearly uniform in the SE depth of escape). It can also be applied to the calculation of the partial yield  $\delta_0$  for incident electrons (Seiler, 1967, Thomas and Pattinson, 1970).

The "transport-albedo" model is an improvement of the classical "infinite medium slowing down" model used by Wolff (1954), Stolz (1959) and more recently by Rösler and Brauer (1981a).

In the "infinite medium slowing down" model, the electron cascade develops in an infinite medium where the internal electron flux  $\Phi_0(E, \mu)$  is uniform. The electrons only escape when the cascade has fully developed. The "transport-albedo" model takes into account the escape of electrons during the cascade.

In plane geometry, the stationary Boltzmann equation for an uniform electron source becomes:

$$\begin{aligned} \mu \frac{\partial}{\partial x} \Phi(x, E, \mu) + \Sigma_s(E) \Phi(x, E, \mu) = \\ \int_{-1}^{+1} \int_{E-1}^{E+1} [\Sigma_s(E' \rightarrow E, \mu' \rightarrow \mu) + \Sigma_s^S(E' \rightarrow E, \mu' \rightarrow \mu)] \cdot \\ \Phi(x, E', \mu') dE' d\mu' + Q(E, \mu) \end{aligned} \quad (11)$$

Since in the "infinite medium slowing down" model, we assume that  $\Phi(x, E, \mu) = \Phi_0(E, \mu)$  is independent of the depth variable, the first term of the left hand side of (11) disappears. To solve (11),  $\Phi_0(E, \mu)$ ,  $Q(E, \mu)$  and  $\Sigma_s(E' \rightarrow E, \mu' \rightarrow \mu) + \Sigma_s^S(E' \rightarrow E, \mu' \rightarrow \mu)$  are expanded in Legendre polynomials.

$$\Phi_0(E, \mu) = \sum_{\ell=0}^{\infty} \frac{2\ell+1}{2} \Phi_{0,\ell}(E) P_{\ell}(\mu) \quad (12)$$

$$Q(E, \mu) = \sum_{\ell=0}^{\infty} \frac{2\ell+1}{2} Q_{\ell}(E) P_{\ell}(\mu) \quad (13)$$

$$\Sigma_s^{(s)}(E' \rightarrow E, \mu' \rightarrow \mu) = \sum_{\ell=0}^{\infty} \frac{2\ell+1}{2} B_{\ell}^{(s)}(E' \rightarrow E) P_{\ell}(\mu) P_{\ell}(\mu') \quad (14)$$

The Boltzmann equation reduces then to a set of independent slowing down equations for each angular order  $\Phi_{0,\ell}(E)$ :

$$\begin{aligned} \Sigma_s(E) \Phi_{0,\ell}(E) = \\ \int_E^{\infty} [B_{\ell}(E' \rightarrow E) + B_{\ell}^S(E' \rightarrow E)] \cdot \Phi_{0,\ell}(E') dE' \\ + Q_{\ell}(E) \end{aligned} \quad (15)$$

Equation (15) can easily be solved by numerical quadrature for each  $\ell$  and the "infinite medium slowing down model" solution  $\Phi_0(E, \mu)$  is obtained using Eq. (12).

The exact internal electron flux  $\Phi(x, E, \mu)$  is not uniform due to the presence of the vacuum-medium interface (with partial reflection boundary conditions). Writing

$$\Phi(x, E, \mu) = \Phi_0(E, \mu) + \Phi_c(x, E, \mu) \quad (16)$$

where  $\Phi_c(x, E, \mu)$  is a flux correction, we have now to solve:

$$\begin{aligned} \mu \frac{\partial}{\partial x} \Phi_c(x, E, \mu) + \Sigma_s(E) \Phi_c(x, E, \mu) = \\ \int_{-1}^{+1} \int_{E-1}^{E+1} [\Sigma_s(E' \rightarrow E, \mu' \rightarrow \mu) + \Sigma_s^S(E' \rightarrow E, \mu' \rightarrow \mu)] \cdot \\ \Phi_c(x, E', \mu') dE' d\mu' \end{aligned} \quad (17)$$

with the following boundary condition:

$$\begin{aligned} \Phi_c(0, E, \mu) = -\Phi_0(E, \mu) \quad 1 \geq \mu \geq \mu_c(E) \\ \Phi_c(0, E, \mu) = \Phi_0(E, -\mu) - \Phi_0(E, \mu) \quad \mu_c(E) \geq \mu \geq 0 \end{aligned} \quad (18)$$

Having expanded  $\Phi_c$  in Legendre polynomials, we introduce in (17) the following approximation:

$$\frac{\Phi_{c,\ell}(x, E')}{\Phi_{0,\ell}(E')} = \frac{\Phi_{c,\ell}(x, E)}{\Phi_{0,\ell}(E)} \quad (19)$$

where  $\Phi_{c,\ell}(x, E')$  are the coefficients of the Legendre expansion of the flux correction.

This approximation assumes that the energy dependence of  $\Phi_{c,\ell}$  for each angular order  $\ell$ , is not influenced by the boundary condition at the surface.

$\Phi_c(x,E,\mu)$  is assumed to be a small correction. Indeed, most internal electrons (free electrons in the target) have very low energies ( $E \ll U_0$ ) and a nearly isotropic angular distribution due to the electron slowing down and multiplication. Hence, the escape cone is very narrow ( $\mu_c(E) \approx 1$ ). The boundary condition is then almost a total reflection boundary condition. Hence, the infinite medium solution is a good approximation and the flux correction should be small and approximation (19) for the flux correction should be used adequately.

Within approximation (19), Eq. (17) reduces to a monoenergetic equation for  $\Phi_c(x,E,\mu)$ :

$$\mu \frac{\partial}{\partial x} \Phi_c(x,E,\mu) + \Sigma_s(E) \Phi_c(x,E,\mu) = \int_{-1}^{+1} f^\dagger(E|\mu' \rightarrow \mu) \Phi_c(x,E,\mu') d\mu' \quad (20)$$

where  $f^\dagger$  is a monoenergetic scattering kernel in which the energy  $E$  appears as a parameter (see (Devooght et al., 1987a). Equation (20) with the ingoing flux boundary condition (18) is a monoenergetic albedo problem which can be solved using the radiative transfer theory of Chandrasekhar (1960). An analytical expression for the solution of this albedo problem has been given by Horak and Chandrasekhar (1961) when the scattering kernel is limited to  $\ell = 2$ . We have used their result and neglected higher order angular terms in our scattering kernel  $f^\dagger$  (Devooght et al., 1987a). Let  $G_s(E, -\mu|E_0, \mu_0)$  be the surface Green's function for the albedo problem, we have:

$$\begin{aligned} \Phi(0,E,-\mu) &= \Phi_0(0,E,-\mu) - \\ &\int_0^\infty \int_0^{+1} G_s(E, -\mu|E_0, \mu_0) \Phi_0(E_0, \mu_0) dE_0 d\mu_0 + \\ &\int_0^\infty \int_0^{+1} G_s(E, -\mu|E_0, \mu_0) \Phi_0(E_0, \mu_0) dE_0 d\mu_0 \end{aligned} \quad (21)$$

The first term of the right-hand side of (21) is the infinite medium solution. The second one is the correction for the semiinfinite character of the problem and the third one is the correction that takes into account the partial reflection of electrons at the boundary.

We first calculate  $\Phi_0(E,\mu)$ . In a second step, we use (21) to correct for the non-uniformity of the flux.

#### Interaction Cross Sections for Polycrystalline Al Targets

In most earlier models, the interactions of electrons in the medium have been described by empirical data. After 1970, several authors have

introduced theoretical models in order to calculate the inelastic (Ganachaud, 1977, Tung and Ritchie, 1977, Rösler and Brauer, 1981a) and elastic mean free paths (Ganachaud, 1977) and the differential cross sections in energy and angle.

The calculation of inelastic mean free paths is based upon the free electron gas model for the interactions of incident particles with the valence electrons. This obviously limits the range of target materials which can be studied with such ab initio calculations. Among these materials, polycrystalline aluminium is the most important. It can be considered as the reference material for experiments and theoretical calculations.

We have used the set of interaction cross sections in polycrystalline Al targets calculated by Ganachaud (1977) (see Dubus et al., 1987).

Polycrystalline aluminium is a radium-jellium (Ganachaud and Cailler, 1979a), i.e. the ionic cores are randomly distributed in the target (Bauer, 1970) (the radium) whereas valence electrons are delocalized and form a free electron gas (the jellium).

Incident particles (electrons or ions) interact inelastically with the free electrons. The screening function is the Lindhard dielectric function (Lindhard, 1954). The interactions of incident particles consist then of two separate contributions: binary encounters and collective excitations (bulk plasmons). We have made the simple assumption that plasmons decay by interband transitions and give rise to one and only one excited electron with an isotropic angular distribution (Dubus et al., 1987). Hence, interactions of incident electrons with the free electron gas give a multiplication of electrons by a factor of two because both the incident and the ejected electrons become part of the cascade while the interactions of incident ions always give rise to one excited electron. The cross section for the binary ion-electron collision is taken from Brice and Sigmund (1980).

Incident electrons and ions interact inelastically with the ionic cores by excitation of core electrons. We have neglected these interactions in our calculations since they do not contribute to SE transport. However, they play an important role as an internal SE source term (Rösler and Brauer, 1981b, 1984, 1988) and for the primary electron transport in the case of incident electrons (Ganachaud, 1977).

Finally, the incident electrons interact elastically with the ionic cores. The interaction potential is the muffin-tin potential of Smrcka (1970).

The inverse mean free paths in polycrystalline Al targets ( $E_f = 11.69$  eV) are shown in Fig. 2, as a function of the internal electron energy. Fig. 2 is similar to Fig. 11 in Ganachaud and Cailler's paper (1979 a) except for the inversion of  $\lambda$ . We have calculated the cross sections using the same interaction model and extended the energy scale up to 2 keV.

All mean free paths show a pronounced minimum at about 45 eV above the bottom of the conduction band. It is seen that elastic scattering is the most prominent interaction process in the energy range below 100 eV.

- 1.Total scattering cross section  $\Sigma_s(E)$
- 2.Elastic cross section
- 3.Inelastic scattering (or creation) cross section
- 4.Plasmon creation cross section
- 5.Binary electron-electron collision cross section

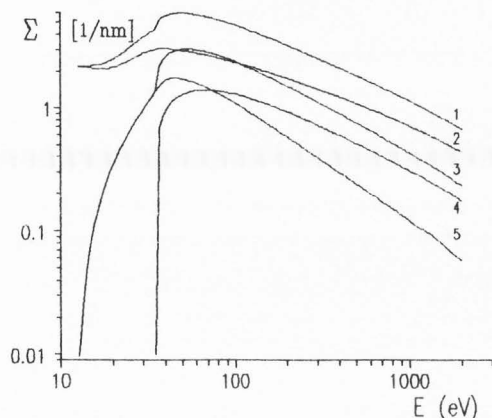


Figure 2. Electron interaction cross sections (inverse mean free paths) in aluminium as a function of internal electron energy E.

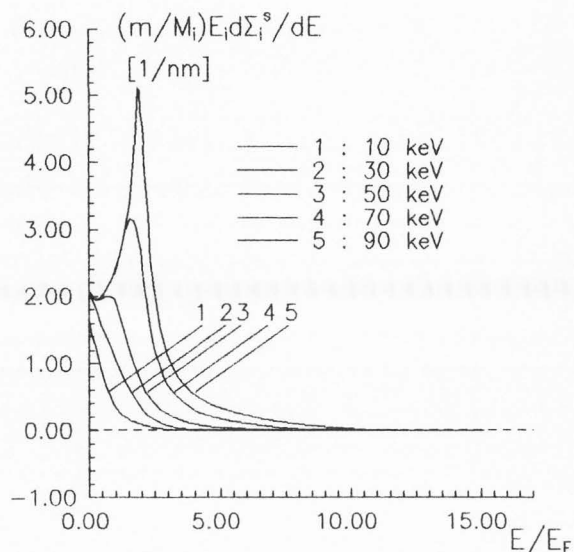


Figure 3. Binary  $H^+$ -electron collision source term calculated using Brice and Sigmund's approximation (1980) in reduced units.

Ganachaud and Cailler (1979a,b) have also considered the excitation of surface plasmons (see for instance (Batson and Silcox, 1983)). We have neglected this process because interactions that take place at the surface cannot be easily incorporated in our transport models. The surface plasmons are responsible for the shoulder seen in the energy spectrum of SE for polycrystalline Al targets (Roepin, 1975, Everhart et al., 1976, Ganachaud, 1977) but their contribution to the electron yield is small.

The binary ion-electron collision source term is shown in Fig.3. Most electrons are created at low energy. Moreover, for high ion energies, a singularity appears in the electron source energy spectrum at about 35 eV above the bottom of the conduction band due to the penetration of the plasmon line in the individual electron excitation zone (Ganachaud, 1977, Pines, 1963).

For incident electrons, the binary electron-electron collision source term shows a similar feature.

We have used in our calculations a realistic and ab initio theoretical set of cross sections. Such a choice is justified by the importance of comparisons of our results with Monte Carlo results (especially the results of Ganachaud, 1977 and Ganachaud and Cailler, 1979b) obtained with similar interaction cross sections.

However, it must be kept in mind that such a realistic treatment of the interaction cross sections is a model and that the possible disagreement between theory and experiment can be due either to the choice of interaction cross sections or to the transport model.

## Results

### "Improved age-diffusion model": incident electron-backward emission (Dubus et al., 1987)

Secondary electron yield The primary electron transport is incorporated in the data for the "improved age-diffusion" model through the internal electron source  $Q(\vec{r}, E, \Omega, t)$  which is given by Eq. (7).

The primary electron flux can be calculated in different ways. An approximate solution of the Boltzmann equation for primary electrons (4) and Monte Carlo calculations are in progress.

We have considered as a simple approximation that the primary electrons have a straight ahead path and slow down according to a semiempirical power law deduced from the range-energy relationships (Kanaya and Kawakatsu, 1972) :

$$r_0 = \begin{cases} 4.259 \times 10^{-2} [E_{p0}(\text{eV})]^{4/3} & \text{A } E_{p0} > 800 \text{ eV} \\ 3.954 \times 10^{-1} [E_{p0}(\text{eV})] & \text{A } E_{p0} < 800 \text{ eV} \end{cases} \quad (22)$$

where  $E_{p0}$  is the incident electron energy.

In order to account for the contribution of backscattered primaries, we have multiplied the calculated yield  $\delta_0$  resulting from the first step by a factor  $(1+\beta\eta)$  according to the well known law of Dobretsov and Matskevitch (1957):

$$\delta = \delta_0(1+\beta\eta) \quad (23)$$

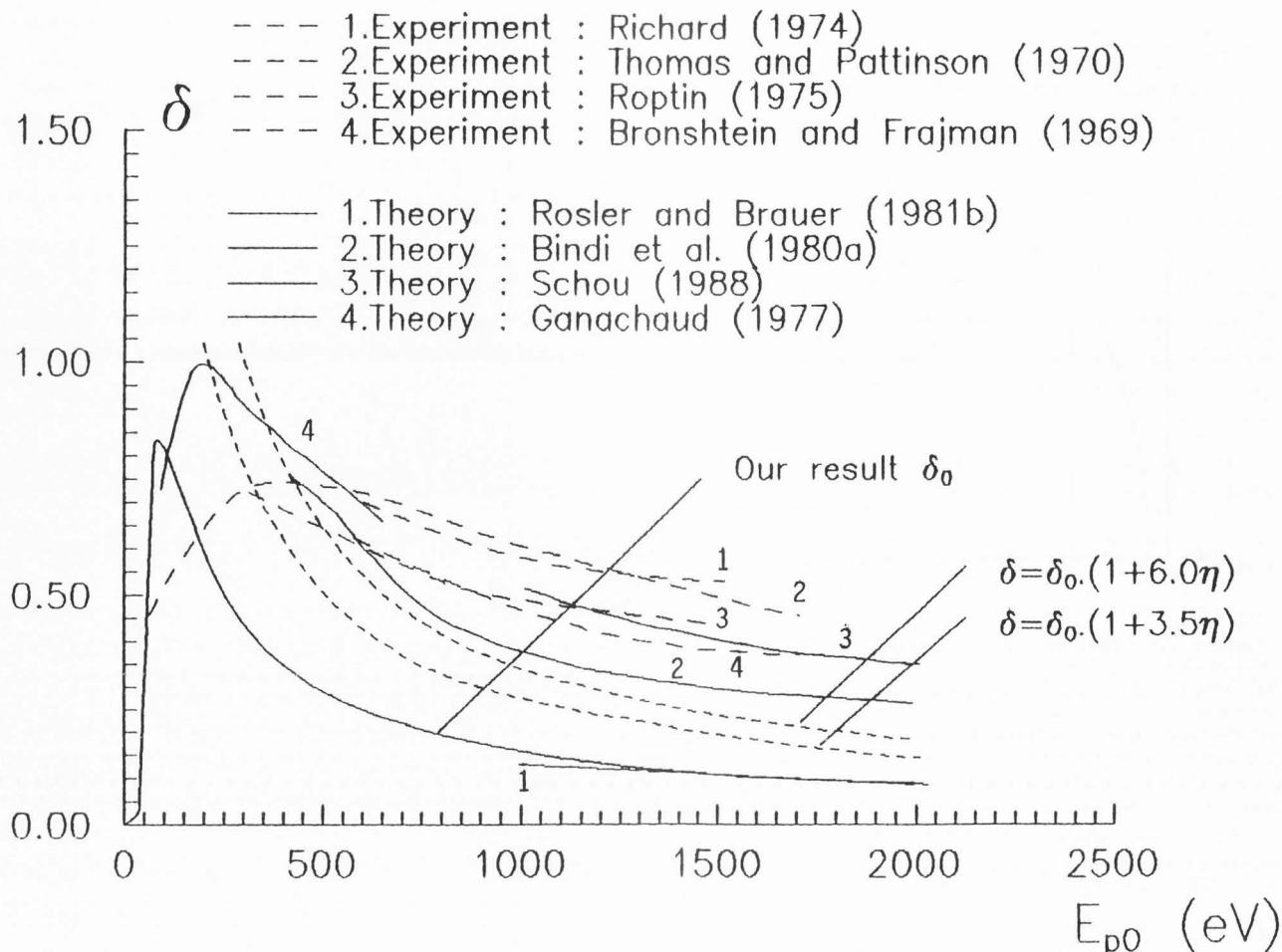


Figure 4. Comparison of our values for the electron yields  $\delta_0$  and  $\delta$  to experimental and other theoretical results.

where  $\eta$  is the yield of backscattered primaries (we have used the experimental values of Roptin, 1975) and  $\beta$  is an empirical coefficient which takes into account the enhancement of the yield due to the backscattered primaries (Thomas and Pattinson, 1970).

We compare in Fig. 4. the electron yield  $\delta_0$  from our model and the yield  $\delta$  corrected for the primary electron backscattering to other theoretical (Rösler and Brauer, 1981b, Ganachaud, 1977, Bindi et al., 1980a, Schou, 1988) and experimental results (Thomas and Pattinson, 1970, Roptin, 1975, Bronshtein and Frajman, 1969, Richard, 1974).

The agreement between our  $\delta_0$  and the results of Rösler and Brauer (1981b) is quite good. However, the correction for the primary electron backscattering using the formula of Dobretsov and Matskevitch (1957) is not very good. Indeed, we have used constant values for  $\beta$  in contradiction with Thomas and Pattinson (1970) who have indicated that  $\beta$  depends on the primary energy.

We compare in Fig. 5. the electron yield  $\delta_0$  calculated with the "improved age-diffusion" model and with a Monte Carlo program. The same microscopic cross sections have been used in both calculations. The agreement is rather good, the

overestimation at low energy ( $E_{p0} \approx 100$  eV) is less than 20%.

The computation of  $\delta$  with the same Monte Carlo program, i.e., taking correctly the primary electron transport and backscattering into account, is in good agreement with experimental results. It can then be assumed that the outgoing electron yield  $\delta$  can be estimated correctly with the "improved age-diffusion" model if one incorporates primary electron transport and backscattering in the internal electron source. This statement is corroborated by the calculations for incident ions (see below).

As has been pointed out above, we have split the internal electron flux in internal primary and internal secondary electrons.

The outgoing electron spectrum consists of a low energy peak ( $E \approx 2$  eV) (the true secondary electrons), a high energy part ( $E \approx E_{p0}$ ) with characteristic losses peaks (the reflected primaries) and a continuous background (see for instance Roptin, 1975). It is usual to consider an electron as a "true secondary" when  $E < 50$  eV and as a "backscattered primary" when  $E > 50$  eV. The total outgoing electron yield  $\sigma$  is split into  $\delta$ , the "true secondary yield" ( $E < 50$  eV) and  $\eta$ , the

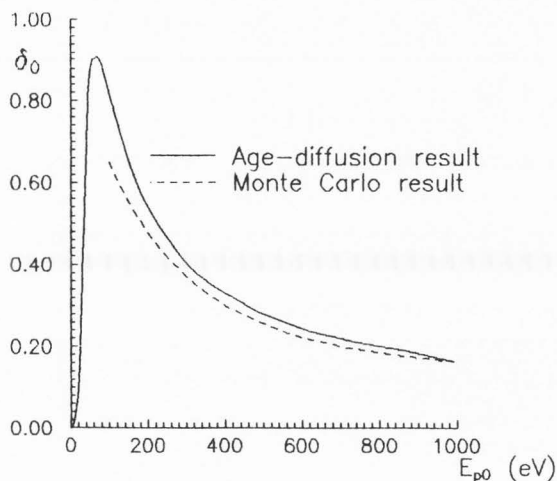


Figure 5. Partial electron yield  $\delta_0$  as a function of the incident electron energy  $E_{p0}$  calculated with the age-diffusion model and with a Monte Carlo code.

"backscattered primary yield" ( $E > 50\text{eV}$ ). This is what we call the experimental use.

Another way of splitting  $\sigma$  into  $\delta$  and  $\eta$  arises from Eq.(3) where the total electron flux  $\Phi_t$  is split into  $\Phi_p$  and  $\Phi$ .

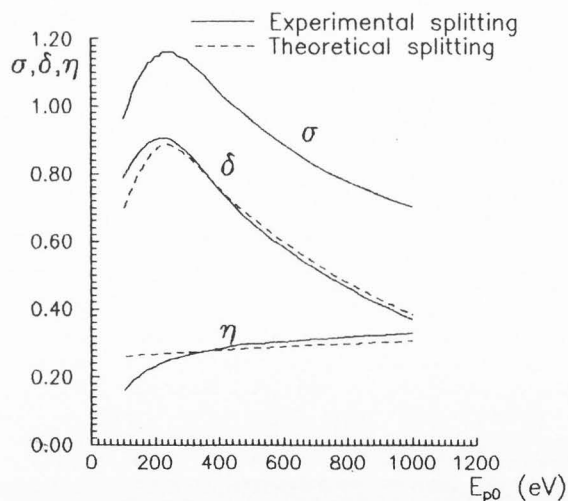


Figure 6. Total electron yield  $\sigma$  calculated with a Monte Carlo code split into  $\delta + \eta$  using both the experimental use and our theoretical convention.

The "backscattering" yield  $\eta$  is the yield of outgoing primaries ( $\Phi_p$ ) while the "true secondary" yield  $\delta$  is the yield of outgoing secondaries ( $\Phi$ ). This is what we call the theoretical "splitting".

With our Monte Carlo program, we have calculated the total yield  $\sigma$  and split it into :

$$\sigma = \delta + \eta \quad (24)$$

We show in Fig.6. the electron yield  $\sigma$  just as  $\delta$  and  $\eta$ , calculated using the "experimental" splitting and the "theoretical" splitting between true secondaries and backscattered primaries. The agreement between both splitting ways is excellent. Moreover, the yield  $\sigma$  calculated with our Monte Carlo program is in good agreement with experimental results (Roptin, 1975).

Energy and angular spectrum of outgoing secondary electrons We compare in Fig.7. the shape of the outgoing electron energy spectrum (normalized at the maximum) calculated with the "improved age-diffusion model" to the experimental result of Roptin (1975) and to the Monte Carlo result of Ganachaud (1977) for  $E_p = 600\text{ eV}$ . Similar comparisons for  $E_p = 300\text{ eV}$  and  $E_p = 1000\text{ eV}$  can be found in Dubus et al. (1987).

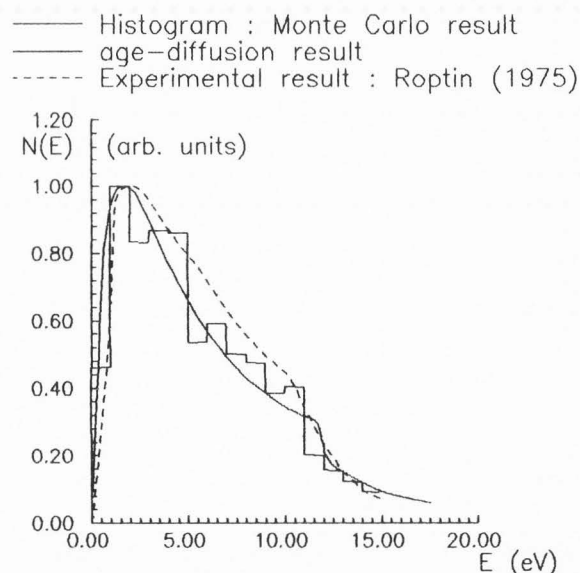


Figure 7. Outgoing electron energy distribution for 600 eV incident electrons on polycrystalline Al targets. Curves are normalized at their maximum.

The spectrum obtained with our model is in good agreement with the Monte Carlo histogram of Ganachaud (1977). The small disagreement with the experimental result can be due to the neglect in our calculations of plasmon decay through multiple electron-hole pairs and of surface plasmon effects which are responsible for a shoulder at 6 eV (Roptin, 1975, Everhart et al., 1976, Chung and Everhart, 1977, Ganachaud, 1977).

The angular distribution of the outgoing

electron current is very close to a cosine distribution which is in good agreement with all experimental evidences and with other theoretical results (see for instance Bronshtein and Frajman, 1969 and Lantéri et al., 1979).

Depth and radial distributions of outgoing secondary electrons The depth distribution of SE is the number of outgoing electrons as a function of the depth of the internal electron source. This depth distribution has a decreasing exponential shape with a characteristic length (averaged over SE energy) of about 10 Å (for  $E_{p0} > 100$  eV). As discussed in Dubus et al. (1987), this supports the assumptions of the earliest models (Baroody, 1950, Bruining, 1954) where electrons are created by the primaries along their paths and escape with an exponential law. In these models, the characteristic length is empirical and independent of both the primary and secondary electron energies. The independence with respect to primary electron energy is confirmed by our calculations. However, it has been shown in Dubus et al. (1987) that this length depends upon the SE energy.

With our Monte Carlo program, the shape of the depth distribution (integrated over SE energy) is nearly a decreasing exponential. The estimated decrease length with Monte Carlo code is 10.8 Å for  $E_{p0} = 300$  eV and 10.7 Å for  $E_{p0} = 1000$  eV.

These results are in quite good agreement with the "improved age-diffusion" results. The energy distribution of outgoing electrons is of course influenced by the depth of the source. This problem is discussed in Dubus et al. (1987) and is due to the slowing down and multiplication process and to the presence of a vacuum-solid interface. For electrons created near the surface, the cascade may be incomplete, i.e., some electrons can escape before they have slowed down. For electrons created far from the surface, the electrons slow down and then can escape through the potential barrier as already pointed out by Koshikawa and Shimizu (1974).

The radial distribution of outgoing electrons is the distribution of the distance of emergence of outgoing SE with respect to the entrance point of the primaries in the target. The shape of this distribution is nearly a two dimensional gaussian distribution. The average value of  $\rho$  is  $\langle \rho \rangle = 14$  Å and is confirmed by a Monte Carlo calculation.

The radial distribution is influenced by the depth of the source. Due to a geometrical effect, the radius at half maximum increases as a function of the source depth and is asymptotically a linear function of the depth.

Time distribution and contributions of the source components The time distribution of outgoing SE is measured with respect to the time the primary particle enters into the target. In the "improved age-diffusion" model, the time distribution is bimodal whereas for Monte Carlo calculations, it is unimodal (see Dubus et al., 1987). This feature is due to the structure of our approximate Green's function which is the sum of two terms with a very different time dependence. The first term represents electrons which escape without slowing down. The second term represents electrons slowing down before they can escape and which are delayed by the slowing down time

(Devooght et al., 1987b, Dubus et al., 1987). The shape of this time distribution is probably wrong due to the age approximation. However, the order of magnitude of the mean outgoing time is correct.

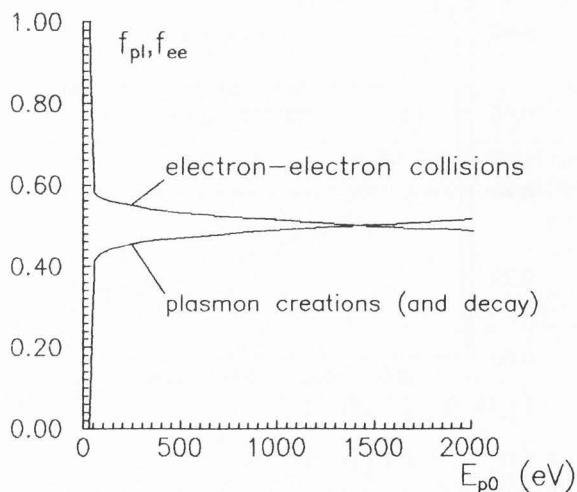


Figure 8. Fraction of outgoing electron resulting from both individual electron excitations and plasmon creations and decays.

We show in Fig. 8 the fraction of the outgoing electrons resulting from the plasmon creations by primary electrons and the fraction of outgoing electrons resulting from individual electron excitations as a function of the incident electron energy. Above the plasmon creation threshold, about 50% of outgoing electrons come from the decay of the plasmons created by the incident electrons while the other 50% come from individual excitations of free electrons. Most internal electrons are created by plasmon decay since the plasmon creation cross section is larger than the binary encounter cross section but the slowing down and multiplication of electrons is much more important for this last contribution. Hence, a similar fraction of outgoing electrons results from plasmon decay and from individual excitations. For Rösler and Brauer (1981b), three times more outgoing electrons result from plasmon creations by the primaries than from individual excitations. The comparison with their results is however difficult since their assumptions for plasmon decay are very different from ours.

Conclusion Except for the time distribution, it is clear that the results obtained with the "improved age-diffusion" model are in very good agreement with Monte Carlo results. If a realistic primary electron transport and surface plasmon excitations are included in the model, the agreement with experiments can be expected to be better. Work in this direction is in progress.

"Improved age-diffusion" model - Incident ions

For incident ions, the charge state of ions in the target must be known in order to calculate the internal electron source. For simplicity, we will limit ourselves to light incident ions, i.e.,  $H^+$  and  $He^{++}$ . We have assumed in our calculations that ions in the target are fully bare ions. This assumption is true for H ions of energy  $E_i > 200\text{keV}$  and for He ions when  $E_i > 800\text{keV}$  (Chateau-Thierry et al., 1976).

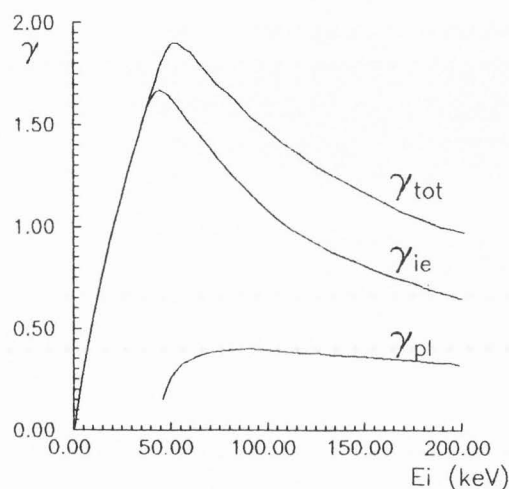


**Figure 9.** Electron yield  $\gamma$  induced by  $H^+$  ions incident on polycrystalline Al targets calculated with the age-diffusion model. The contribution of individual (ie) and collective (pl) excitations are represented.

Electron yield We show in Fig. 9 the outgoing electron yield  $\gamma$  as a function of  $H^+$  incident energy. The electron yield is split into the binary collision source term and the plasmon source term. The position of the maximum, i.e.,  $E(H^+) \approx 55\text{keV}$  and the order of magnitude of the yield are in good agreement with experimental data (see Dubus et al., 1986, Baragiola et al., 1979, Svensson and Holmen, 1982, Hasselkamp et al., 1981). The fraction of outgoing electrons resulting from individual electron excitations by the incident ions is at least two times the fraction resulting from plasmon creations; while for Rösler and Brauer (1984) the fraction resulting from plasmon creations is larger than the fraction resulting from individual electron excitations for  $E_i > 150\text{keV}$ . Once again, for the splitting into the components of the source, the comparison with the results of Rösler and Brauer is difficult since their assumptions for plasmon decay are not the same as ours.

"Transport-albedo" model - Incident ions

Electron yield We show in Fig. 10 the electron yield  $\gamma$  as a function of incident  $H^+$  energy.

We compare the theoretical electron yield obtained in the "infinite medium slowing down" model and in the "transport-albedo" model to experimental results (Baragiola et al., 1979, Svensson and Holmen, 1982, Hasselkamp et al., 1981). The agreement between theoretical and experimental results is good up to 100 keV. For higher energy, the disagreement can be due to the neglect in our calculations of the inner-shell ionizations. It is worth noting that our results could be improved if we correctly take the charge state of ions in the target into account. The surface correction, i.e., the reduction factor of the yield due to the presence of the vacuum-medium interface with partial reflection boundary conditions is about 0.85 (for  $l = 1$ ) and 0.8 (for  $l = 2$ ) ( $l$  is the maximum angular order of the "monoenergetic" scattering kernel  $f^{\dagger}$  in our calculations (see above)).

This last value is not modified by the inclusion of  $l = 3$  terms in the correction at angular order  $l = 2$ . Moreover, comparisons with Monte Carlo calculations confirm this value. Hence we expect that the "transport-albedo" model gives the good value of the surface correction and that the "infinite medium slowing down" model overestimates the electron yield by about 20%.

Outgoing electron energy spectrum We compare in Fig. 11 the absolute energy distribution of electrons emitted backwards for 200 keV incident  $H^+$  ions obtained with the "infinite medium slowing down" model and the "transport-albedo" model to the experimental results of Hasselkamp and Scharmann (1983a). The agreement between theory and experiment is fair although not excellent. The inclusion of surface plasmons in our calculations could perhaps improve the agreement. The surface correction calculated as a function of the outgoing electron energy is 1 when  $E = 0\text{eV}$  and decreases to about 0.6 when  $E \approx 50\text{eV}$ . For very low electron energies, the surface is almost perfectly reflecting (which explains the low values of the surface correction), while for high electron energies, the surface is almost perfectly absorbing (which explains lower values of the surface correction).

Forward to backward yield ratio and influence of the tilt angle of the target For thin targets, primary particles can be transmitted through the target and secondary emission takes place both in the forward and in the backward directions (Meckbach et al., 1975). For the specific case of beam foil conditions (100 keV  $H^+$  ions incident on  $10\ \mu\text{g}/\text{cm}^2$  carbon foils for instance), the energy loss of ions in the target (maximum 10%) can be neglected in a first approximation. The angular dispersion of ions in the target can be responsible for an increase of the forward yield but it will be neglected. The internal electron source is then the same for the forward and backward emissions. Only the anisotropy of the source is responsible, in our model, for a forward to backward yield ratio

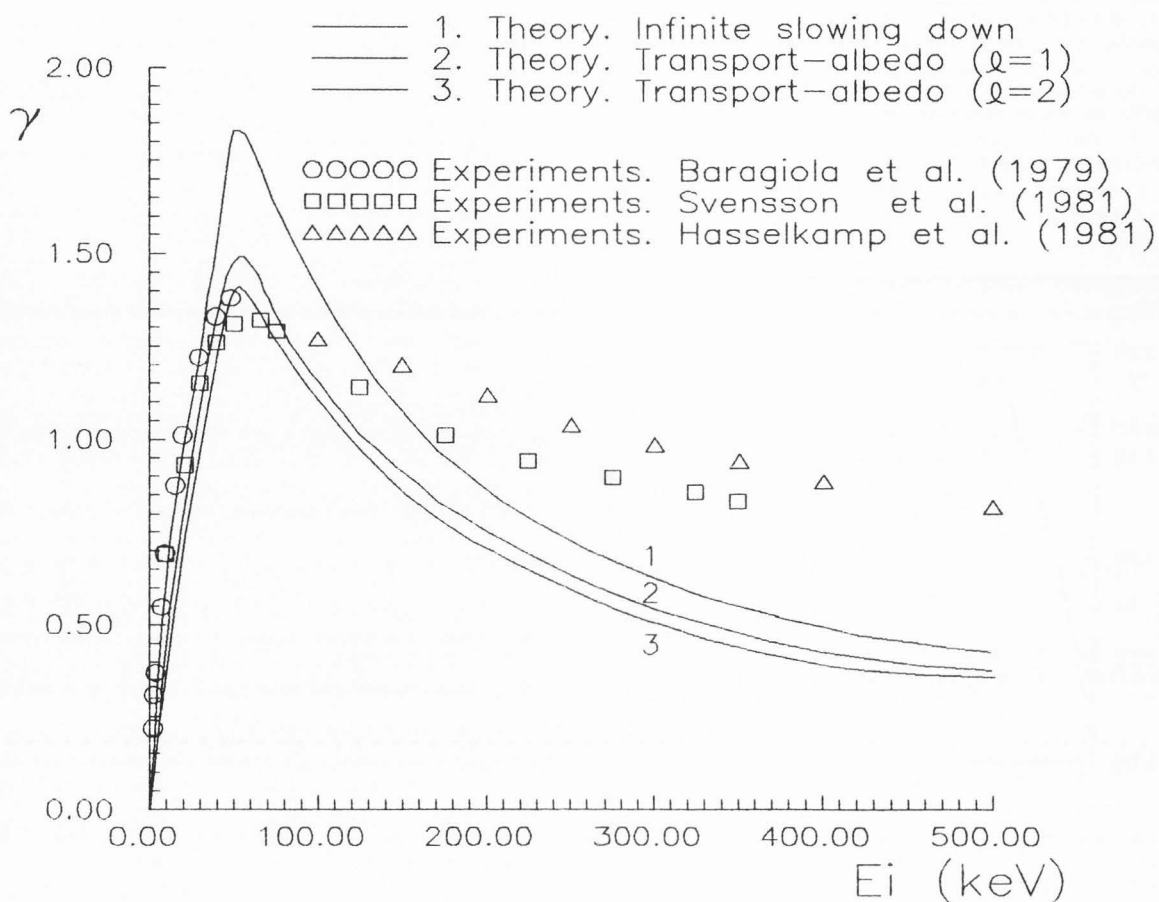


Figure 10. Backward electron yield  $\gamma_B$  for  $H^+$  ions incident on polycrystalline Al targets. Theoretical results are compared to experiments.

$R_Y = Y_F / Y_B$  larger than 1. We have calculated the forward to backward yield ratio  $R_Y$  with the "improved age-diffusion" model, with the "infinite medium slowing down" model and with the "transport-albedo" model. We compare in Fig.12 our theoretical results for  $H^+$  incident ions to the experimental results of Meckbach et al. (1975).

The results of Meckbach et al. (1975) have been criticized by Hasselkamp and Scharmann (1983b) because there is no maximum in the electron yield as a function of  $H^+$  energy.

The results of Meckbach for  $R_Y$  have however been reproduced in similar experimental conditions in Brussels (Dehaes and Carmeliet, private communication) with a maximum for the electron yield at about 80 keV.

There is an obvious disagreement between experimental and theoretical results. Meckbach's result has been obtained for thin carbon foils and our theoretical results have been obtained for Al targets. The poor vacuum conditions in the experiments or phenomena such as the capture and loss mechanisms in the target may influence the anisotropy. Experiments in ultra-high-vacuum

conditions and calculations which take into account all mechanisms that could influence the forward to backward yield ratio have to be performed.

The influence of the tilt angle of the target is an interesting feature of SEE. Simple geometrical considerations lead to a dependence of the electron yield (forward+backward) in  $1/\cos\theta$  where  $\theta$  is the tilt angle.

Such a simple law is generally correct for backward emission induced by incident protons on thick targets (Svensson et al., 1981).

For heavier elements, deviations with respect to the  $1/\cos\theta$  law are evidenced experimentally. Most authors have used a  $(1/\cos\theta)^n$  law (Svensson et al., 1981) in order to characterize the deviation with respect to the  $1/\cos\theta$  law ( $n$  is an adjustable parameter).

For the total electron yield (forward + backward) induced by ions incident on thin carbon foils, Garnir et al. (1982) have used a :

$$\gamma(\theta) = \gamma(0) [ A + (1-A)/\cos\theta ] \quad (25)$$

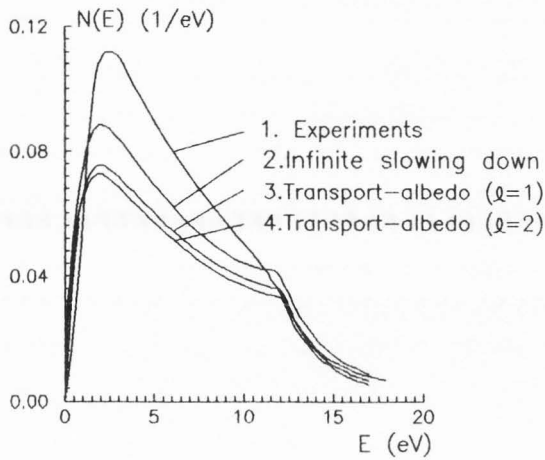


Figure 11. Outgoing electron energy distribution for 200 keV  $H^+$  ions incident on polycrystalline Al targets.

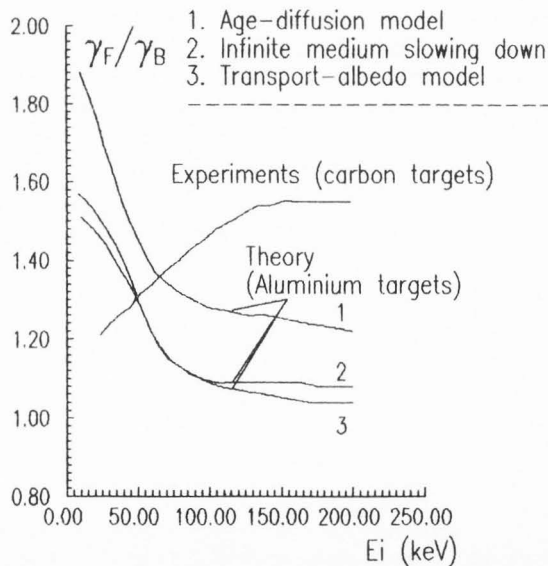


Figure 12. Forward to backward yield ratio for  $H^+$  ions incident on polycrystalline Al targets (theory). The experimental result is for amorphous carbon targets.

law due to the excellent linear behaviour of  $\langle \theta \rangle$  as a function of  $1/\cos\theta$ .

We have considered theoretically the influence of the anisotropy of the production of internal electrons on the dependence of the yield as a function of the tilt angle and have obtained for the first angular terms ( $l \leq 2$ ):

$$\gamma(\theta) = \gamma(0) [A / \cos \theta + B \cos \theta] \quad (26)$$

The independent term has disappeared since the source is, in our calculations, the same for the forward and backward emissions and since the yield that we consider is the sum of  $\gamma_F$  and  $\gamma_B$ .

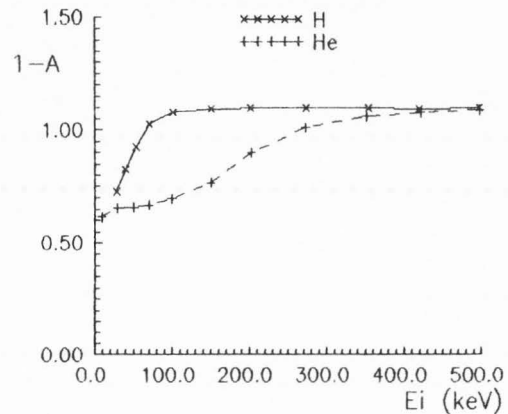


Figure 13.  $1-A$  parameter obtained by adjusting the infinite slowing down results for the influence of the tilt angle to formula (25).

Adjusting our theoretical results to the formula of Garnir et al. (1982), we have obtained  $A$  values which are shown in Fig. 13 for  $H^+$  and  $He^{++}$  ions incident on polycrystalline Al targets.  $A$  takes values between 0.4 and -0.1 while the values of Garnir are between 0.7 and 0.3 for  $He^+$  ions incident on thin carbon foils. It is impossible to draw any conclusions since target materials are not the same and since we didn't take into account the electron capture and loss processes in the solid. It is however worth noting that, as is shown in our calculations, the anisotropy of the production of internal electron can be responsible for  $A$  values different from 0.

Electron yield and electronic stopping power for  $H^+$  ions incident on polycrystalline Al targets We give in Table I the ratio of the backward electron yield calculated with the "infinite medium slowing down" and the "transport-albedo" models and the electronic stopping power calculated using the same cross-sections for  $H^+$  ions incident on

polycrystalline Al targets.

$\gamma_B / S_e$  is approximately 0.011 nm/eV for the "infinite medium slowing down" model and 0.0095 nm/eV for the "transport-albedo" model and is nearly independent of the incident ion energy. These results are in good agreement with the experimental values of Hasselkamp (1985) (0.0116 nm/eV ( $\pm 11.3\%$ )). Brauer and Rösler (1985) obtain  $\gamma_B / S_e$  values ranging from 0.0082 nm/eV for 40 keV incident  $H^+$  ions to 0.0037 nm/eV for 800 keV incident  $H^+$  ions.

Conclusion It appears that, for incident ions, the agreement between the results obtained with the "transport-albedo" model and experiments is rather good. However, for the forward to backward yield ratio and the influence of the tilt angle of the target, some problems remain which have to be solved in the future.

#### Comparisons of our Models with other Electron Emission Models

We present here a brief comparison between our models and the other microscopic models, i.e., the Monte Carlo calculations, the  $S_N$ -multigroup and the "infinite medium slowing down" model. This comparison only considers technical aspects of the transport models. Thereafter we compare briefly the microscopic emission models with Schou's model (1980a,b).

#### Comparisons between microscopic models

Monte Carlo can be considered apart from the numerical solutions of the Boltzmann equation. The first advantage of Monte Carlo calculations is the large versatility of the method, i.e., one can easily modify the program in order to account for oblique incidences, surface plasmon processes, etc. Another advantage of Monte Carlo with respect to other transport methods is that all variables, for instance energy, angle, time, radial position are obtained. Lastly, no approximation is made in the transport process (in the frame of the radium model of course (Bauer, 1970)). The Monte Carlo calculations can then be considered as a reference when we compare results obtained with different transport methods but with the same interaction model. The inconvenience is that Monte Carlo is time consuming and cannot therefore be used for a parametric study of SEE.

$S_N$ -multigroup is a direct numerical solution of the Boltzmann equation. Angle, energy and space variables are discretized. Unfortunately, this method requires a large amount of computer memory and is time consuming, especially if accurate results are needed.

As the Monte Carlo method, this transport method is exact except for the discretization of the Boltzmann equation. However, with respect to Monte Carlo calculations, the versatility of such a method is not excellent. It is difficult to extend the spatial problem to 2 or 3 dimensions, the time variable cannot be included easily, etc.

Compared to Monte Carlo and  $S_N$ -multigroup, the "infinite medium slowing down" model, the "transport-albedo" model and the "improved age-diffusion" model give approximate solutions of the transport problem and use as input data the internal electron source. Monte Carlo and  $S_N$ -

**Table I.** Electron yield  $\gamma$  for  $H^+$  ions incident on polycrystalline Al targets obtained with the "infinite medium slowing down" (is) and the transport-albedo ( $l=1$ ) (ta) models scaled to the electronic stopping power  $S_e=(dE/dx)_e$ .

$E_H^+$ keV	$\gamma_{is}$	$\gamma_{ta}$	$S_e$ eV/nm	$\gamma_{is}/S_e$ nm/eV	$\gamma_{ta}/S_e$ nm/eV
10	0.55	0.47	53.1	0.0104	0.0089
30	1.11	0.94	96.1	0.0115	0.0098
50	1.56	1.31	136.0	0.0114	0.0096
70	1.44	1.23	126.4	0.0114	0.0097
100	1.20	1.03	107.0	0.0112	0.0096
150	0.92	0.80	84.7	0.0110	0.0095
200	0.76	0.66	71.2	0.0106	0.0092
500	0.38	0.34	36.3	0.0105	0.0094

multigroup calculations use either an internal electron source or an ingoing electron flux as input data.

The "infinite medium slowing down" and the "transport-albedo" models can only be applied to problems where the internal electron source is homogeneous (or almost constant in the SE escape depth). The energy variable is emphasized and the energy and angular spectrum of outgoing electrons are well predicted. However, all other variables are omitted and we have no information about what happens in the target. The "transport-albedo" model improves the infinite medium slowing down model since it takes into account the boundary conditions at the interface.

Finally, the "improved age-diffusion" model is an approximate model which is rather versatile since it allows an arbitrary internal electron source, gives the radial and time distributions, etc. All variables are treated on an equal footing, i.e., with a reasonable precision. It allows a parametric study because it is not time consuming. Comparisons between Schou's model (1980a,b) and microscopic models

The fundamental difference between Schou's theory and microscopic models can be found in the classical splitting of the emission process into three stages.

For Schou's model, the first step of the emission process incorporates both the primary particle penetration with the internal electron production and the secondary ionization by energetic secondary electrons (Schou, 1988). Part of the transport process is incorporated in this first stage of the emission process and the data for Schou's model are the energy deposition at the surface and the electron stopping power in the material. These macroscopic data incorporate the electron interaction cross sections and the

electron cascade in the target.

Hence, all problems arising, for the microscopic models, from the choice of realistic cross sections and from the description of electron multiplication and transport disappear. It is, in that sense, more usable than microscopic models since it can be applied to both electron and ion induced SEE and to any combination of incident particles and targets. The microscopic models are very dependent on the realistic description of the microscopic interactions in the material.

Schou's model is a quite practical model of SEE that can be used in many cases but when one wants to study with some precision a particular aspect of SE, microscopic models have to be used.

### Conclusion

We have given, in this paper a brief overview of the work that has been done in Brussels about SEE. We have described the results that have been obtained with the "improved age-diffusion" and the "transport-albedo" models. These results compare fairly well to the results of the most evolved microscopic models for SEE, i.e. the models of Ganachaud and Cailler (1979a,b), Bindi et al. (1980a,b,c), and Rösler and Brauer (1981a,b). The "improved age-diffusion" model is designed for a parametric study of electron transport due to its analytical aspect whereas the "transport-albedo" model is an improvement of the "infinite medium slowing down" model used by Rösler and Brauer (1981a,b). Compared to the model of Schou (1980a,b), our models have advantages and disadvantages which have been discussed more extensively.

A comparison between the existing electron transport models, i.e., Monte Carlo calculations, the "infinite medium slowing down" model,  $S_N$ -multigroup, the "improved age-diffusion" and "transport-albedo" models has still to be done. Work is now in progress in order to compare our models with Monte Carlo calculations.

Some problems resulting from physical assumptions remain, especially for incident ions. The forward to backward yield ratio and the influence of the tilt angle are features which are not well described. We have calculated the influence of the anisotropy of the internal electron source on these characteristics. Other physical phenomena could influence these characteristics and more work has still to be done.

Finally, for incident electrons, a realistic treatment of primary electron transport must be incorporated in the calculation of the internal electron source in order to give a correct electron yield.

### Table of symbols

SE :	Secondary Electron(s)
SEE :	Secondary Electron Emission
IIEE :	Ion Induced Electron Emission
a.u. :	atomic units
H(x) :	Heaviside step function
$\delta(x)$ :	delta function
$U_0$ (eV) :	Height of the potential barrier at the vacuum-medium interface
$E_F$ (eV) :	Fermi energy
$\vec{r}$ (m) :	position vector
$v, E$ (m/s, eV) :	velocity, energy (in the solid)
$\vec{\Omega}, t$ (s) :	direction vector and time variable for internal electrons
$x, \mu, \bar{\rho}$ :	depth variable, angle variable in plane geometry and radial position vector of electrons
$\vec{I}_x$ :	inward normal to the surface
$N_{p0}, \mu_{p0}, E_{p0}, \bar{\Omega}_{p0}$ :	incident electron number, director cosine, energy and direction vector for incident electrons
$J_i, \mu_i, E_i, \bar{\Omega}_i$ :	incident ion current, director cosine, energy, direction vector for incident ions
$\Phi_t(\vec{r}, E, \bar{\Omega}, t)$ :	total electron flux for incident electrons
$\Phi_p(\vec{r}, E, \bar{\Omega}, t)$ :	primary electron flux for incident electrons
$\Phi(\vec{r}, E, \bar{\Omega}, t)$ :	internal secondary electron flux
$\Phi_i(\vec{r}, E, \bar{\Omega}, t)$ :	ion flux for incident ions
$Q(\vec{r}, E, \bar{\Omega}, t)$ :	internal secondary electron source
$\mu_c(E)$ :	critical cosine for escape
$E_{min}$ (eV) :	minimum energy for an ion creating an electron of energy E
$\Sigma_s(E)$ :	scattering cross section for internal electrons
$\Sigma_s(E \rightarrow E, \bar{\Omega} \rightarrow \bar{\Omega})$ :	differential "scattering" cross section
$\Sigma_s^s(E \rightarrow E, \bar{\Omega} \rightarrow \bar{\Omega})$ :	differential "creation" cross section
$\Sigma_i(E \rightarrow E, \bar{\Omega} \rightarrow \bar{\Omega})$ :	differential "creation" cross section for incident ions
$\Phi_0(\vec{r}, E, t)$ :	isotropic part of the internal electron flux (age-diffusion model)
$Q_0(\vec{r}, E, t)$ :	isotropic part of the internal electron source
$\vec{Q}_1(\vec{r}, E, t)$ :	current vector of the internal electron source
$D(E)$ :	diffusion coefficient (age-diffusion model)
$\Sigma_0(E)$ :	effective absorption cross section (age-diffusion model)
$\Sigma_{Rem}(E)$ :	removal cross section (age-diffusion model)
$\phi(x, E, \mu)$ :	internal electron flux in plane geometry
$Q(E, \mu)$ :	uniform internal electron source in

plane geometry	
$\Phi_0(E, \mu)$	: infinite medium slowing down flux
$\Phi_c(x, E, \mu)$	: flux correction in the transport-albedo model
$\Sigma_s(E \rightarrow E, \mu \rightarrow \mu)$	: differential "scattering" cross section in plane geometry
$\Sigma_s^s(E \rightarrow E, \mu \rightarrow \mu)$	: differential "creation" cross section in plane geometry
$\Phi_l(x, E)$	: Legendre development terms of the internal electron flux
$Q_l(x, E)$	: Legendre development terms of the internal electron source
$B_l(E \rightarrow E)$	: angular moments of the differential scattering cross section
$B_l^s(E \rightarrow E)$	: angular moments of the differential creation cross section
$\Phi_{c, l}(x, E)$	: angular moments of the flux correction
$f^s(E   \mu \rightarrow \mu)$	: monoenergetic scattering kernel (transport-albedo model)
$G_s(E, -\mu   E_0, \mu_0)$	: Surface Green's function for the monoenergetic albedo problem
$\sigma$	: total outgoing electron yield for incident electrons
$\delta$	: true secondary yield for incident electrons
$\eta$	: yield of backscattered primaries for incident electrons
$\delta_0$	: partial electron yield for incident electrons due to forward primary electrons
$\beta$	: efficiency coefficient of electron emission for backscattered primaries
$f_{pl} + f_{ee}$	: fractions of true secondary electrons due respectively to the plasmon creation (and decay) and binary encounter processes for incident electrons
$\gamma$	: electron yield for incident ions
$\gamma(\theta)$	: electron yield for incident ions as a function of the tilt angle of the target
$\gamma_F \gamma_B$	: Forward and backward yields for ions incident on thin targets
$R_\gamma$	: forward to backward yield ratio

## References

- Austin L., Starke H. (1902) "Über die Reflexion der Kathodenstrahlen und eine damit verbundene neue Erscheinung sekundärer Emission" *Ann Phys.* **9**, 271-292.
- Baragiola R.A., Alonso E.V., Oliva Florio A. (1979) "Electron emission from clean metal surfaces induced by low-energy light ions" *Phys. Rev.* **B19**, 121-129.
- Baroody E.M. (1950) "A theory of secondary electron emission from metals" *Phys. Rev.* **78**, 780-787.
- Batson P.E., Silcox J. (1983) "Experimental energy-loss function,  $\text{Im}[-1/\epsilon(q, \omega)]$ , for aluminium" *Phys. Rev.* **B27**, 5224-5239.
- Bauer E. (1970) "Interaction of slow electrons with surfaces" *J. Vac. Sci. Technol.* **7**, 3-13.
- Bethe H.A. (1941) "On the theory of secondary emission" *Phys. Rev.* **59**, 940-940.
- Bindi R., Lantéri H., Rostaing P. (1980a) "A new approach and resolution method of the Boltzmann equation applied to secondary electron emission, by reflection from polycrystalline aluminium" *J. Phys. D: Appl. Phys.* **13**, 267-280.
- Bindi R., Lantéri H., Rostaing P. (1980b) "Application of the Boltzmann equation to secondary electron emission from copper and gold" *J. Phys. D: Appl. Phys.* **13**, 461-470.
- Bindi R., Lantéri H., Rostaing P., Keller P. (1980c) "Theoretical efficiency of backscattered electrons in secondary electron emission from aluminium, *J. Phys. D: Appl. Phys.* **13**, 2351-2361.
- Bindi R., Lantéri H., Rostaing P. (1987) "Secondary electron emission induced by electron bombardment of polycrystalline metallic targets" *Scanning Microscopy*, **1**, 1475-1490.
- Bishop H.E., Chornik B., LeGressus C., LeMoel A. (1984) "Crystalline effects in Auger electron spectroscopy", *Surf. Interf. Anal.* **6**, 116-128.
- Brauer W., Rösler M. (1985) "On the relation between stopping power and proton-induced electron emission for intermediate energies: Aluminium" *Phys. Stat. Sol. (b)* **131**, 177-183.
- Brice D.K., Sigmund P. (1980) "Secondary electron spectra from dielectric theory" *Kgl. Danske Videnskab Selskab Mat. Fys. Medd.* **40**, 1-34.
- Bronshstein I.M., Frajman B.S. (1969) "Secondary Electron Emission" (in Russian) Ed. Nauka, Moscow.
- Bruining H. (1954) "Physics and Applications of Secondary Electron Emission" Pergamon Press Ltd., London.
- Chandrasekhar S. (1960) "Radiative Transfer" Dover Publications Inc., New York.
- Chateau-Thierry A., Gladieux A., Delaunay B. (1976) "Experimental neutral charge fractions in proton beams emerging from solids" *Nucl. Instr. Meth.* **132**, 553-558.
- Chung M.S., Everhart T.E. (1977) "Role of plasmon decay in secondary electron emission in the nearly-free-electron metals. Application to aluminium" *Phys. Rev.* **B15**, 4699-4715.
- Devooght J., Dehaes J.C., Dubus A., Hollasky N. (1984) "A time dependent secondary electron transport model" in "Forward Electron Ejection in Ion Collisions", Proceedings, Aarhus, Denmark, 1984, edited by K.O. Groeneveld, W. Meckbach and I.A. Sellin, Springer-Verlag, Berlin, p.52-61.

- Devooght J., Dubus A., Dehaes J.C. (1987a) "Semianalytical theory of ion induced secondary electron emission and transport in semiinfinite media" in the Proceedings of the "International Topical Meeting on Advances in Reactor Physics, Mathematics and Computation", Paris, 1987, edited by ANS/ENS/SFEN, p. 339-349.
- Devooght J., Dubus A., Dehaes J.C. (1987b) "Improved age-diffusion model for low-energy electron transport in solids. I. Theory" *Phys. Rev. B36*, 5093-5109.
- Dobretsov L.N., Matskevitch T.L. (1957) "The role of reflected electrons in secondary electron emission", *Sov. Phys.-Tech. Phys.* 2, 663-672.
- Dubus A., (1987) Application de Méthodes de Neutronique au Transport d'Electrons à Basse Energie dans les Solides et Notamment à l'Emission d'Electrons Secondaires., PhD Thesis, Université Libre de Bruxelles, Belgium.
- Dubus A., Devooght J., Dehaes J.C. (1986) "A theoretical evaluation of ion induced secondary electron emission" *Nucl. Instr. Meth.* B13, 623-626.
- Dubus A., Devooght J., Dehaes J.C. (1987) "Improved age-diffusion model for low-energy electron transport in solids. II. Application to secondary emission from aluminium" *Phys. Rev.* B36, 5110-5119.
- Eckstein W., Verbeek H. (1984) "Reflection of light ions from solids" in Data Compendium for Plasma-Surface Interactions", *Nucl. Fus. Special Issue*, 12-28.
- Everhart T.E., Hoff P.H. (1971) "Determination of kilovolt electron energy dissipation vs. penetration distance in solid materials", *J. Appl. Phys.* 42, 5837-5846.
- Everhart T.E., Saeki N., Shimizu R., Koshikawa T. (1976) "Measurement of structure in the energy distribution of slow secondary electrons from aluminium" *J. Appl. Phys.* 47, 2941-2945.
- Ferziger J.H., Zweifel P.F. (1966) "The theory of neutron slowing-down in nuclear reactors" Pergamon Press, Oxford.
- Ganachaud J.P. (1977) "Contribution à l'étude théorique de l'émission électronique secondaire des métaux" PhD Thesis, Université de Nantes, France.
- Ganachaud J.P., Cailler M. (1979a) "A Monte-Carlo calculation of the secondary electron emission of normal metals, I, The model" *Surf. Sci.* 83, 498-518.
- Ganachaud J.P., Cailler M. (1979b) "A Monte-Carlo calculation of the secondary electron emission of normal metals, II, Results for aluminium" *Surf. Sci.* 83, 519-530.
- Garnir H.P., Dumont P.D., Baudinet-Robinet Y. (1982) "Secondary electron emission from thin foils under fast ion bombardment" *Nucl. Instr. Meth.* 202, 187-192.
- Gay T.J., Berry H.G. (1979) "Temperature dependence of alignment production in He<sup>1</sup> by beam-foil excitation" *Phys. Rev.* A19, 952-961.
- Hasselkamp D., Lang K.G., Scharmann A., Stiller N. (1981) "Ion induced electron emission from metal surfaces" *Nucl. Instr. Meth.* 180, 349-356.
- Hasselkamp D., Scharmann A. (1983a) "Die Sekundärelektronenemission von Aluminium beim Beschuss mit H<sup>+</sup>, He<sup>+</sup>, Ne<sup>+</sup> und Ar<sup>+</sup>-Ionen im Energiebereich von 100 keV bis 800 keV: Teil II" *Vakuumtechnik* 32, Heft 1, 9-16.
- Hasselkamp D., Scharmann A. (1983b) "Ion-induced electron emission from carbon" *Phys. Stat. Sol.* (a) 79, K197-K200.
- Hasselkamp D. (1985) "Die Ioneninduzierte Kinetische Elektronenemission von Metallen bei Mittleren und Grossen Projektilenergien" Habilitationsschrift, Thesis, Giessen, Germany.
- Horak H.G., Chandrasekhar S. (1961) "Diffuse reflection by a semi-infinite atmosphere" *Astrophys. J.* 134, 45-56.
- Kanaya K., Kawakatsu H. (1972) "Secondary electron emission due to primary and backscattered electrons" *J. Phys. D: Appl. Phys.* 5, 1727-1742.
- Koshikawa T., Shimizu R. (1974) "A Monte Carlo calculation of low-energy secondary electron emission from metals" *J. Phys. D:Appl. Phys.* 7, 1303-1315.
- Lantéri H., Bindi R., Rostaing P. (1979) "Application de l'équation de Boltzmann à la transmission d'électrons et à l'émission électronique secondaire" *Vide* 196, 79-93.
- Lantéri H., Bindi R., Rostaing P. (1982) "Modèle théorique de la transmission et de la rétrodiffusion d'électrons dans des cibles métalliques minces ou semi-infinies: Application à l'aluminium, l'argent et le cuivre" *Thin Solid Films* 88, 309-333.
- Lantéri H., Rostaing P., Bindi R. (1986), Application du modèle théorique à l'étude des pertes d'énergie caractéristiques des électrons transmis et rétrodiffusés dans le cas de l'aluminium, *Thin Solid Films* 135, 289-299.
- Lindhard J. (1954) "On the properties of a gas of charged particles" *Kgl. Danske Videnskab Selskab Mat. Fys. Medd.* 28, 1-57.
- Meckbach W., Braunstein G., Arista N. (1975) "Secondary-electron emission in the backward and forward directions from thin carbon foils traversed by 25-250 keV proton beams" *J. Phys. B: Atom. Molec. Phys.* 8, L344-L349.
- Pines D. (1963) "Elementary excitations in solids" W.A. Benjamin Inc., New York.
- Richard C. (1974) "Contribution à l'étude de l'émission électronique secondaire par bombardement électronique, sur des cibles d'Al et Au", Thèse de Spécialité, Université de Provence, France.
- Roptin D. (1975) "Etude expérimentale de l'émission électronique secondaire de l'Aluminium et de l'Argent" Thèse de Docteur-Ingénieur, Université de Nantes, France.
- Rösler M., Brauer W. (1981a) "Theory of secondary electron emission. I. General theory for nearly-free-electron metals" *Phys. Stat. Sol.* (b) 104, 161-175.
- Rösler M., Brauer W. (1981b) "Theory of secondary electron emission. II. Application to aluminium" *Phys. Stat. Sol.* (b) 104, 575-587.
- Rösler M., Brauer W. (1984) "On the theory of ion-induced electron emission" *Phys. Stat. Sol.* (b) 126, 629-642.
- Rösler M., Brauer W. (1988) "Theory of electron emission from solids by proton and electron bombardment" *Phys. Stat. Sol.* (b) 148, 213-226.
- Rostaing P., Bindi R., Lantéri H. (1986) "Modèle théorique pour l'analyse des différents processus de diffusion des électrons dans les métaux" *Thin Solid Films* 135, 277-287.

Schou J. (1980a) "Transport theory for kinetic emission of secondary electrons from solids" Phys. Rev. **B22**, 2141-2174.

Schou J. (1980b) "Transport theory for kinetic emission of secondary electrons from solids by electron and ion bombardment" Nucl. Instr. Meth. **170**, 317-320.

Schou J. (1988) "Secondary electron emission from solids by electron and proton bombardment" Scanning Microscopy. **2**, 607-632.

Schou J. (1989) "Secondary electron emission: progress and prospects". Scanning Microscopy **3**, 429-433.

Seiler H. (1967) "Einige aktuelle Probleme der Sekundärelektronenemission" Z. Angew. Phys. **[22]3**, 249-263.

Sigmund P., Tougaard S. (1981) "Electron emission from solids during ion bombardment. Theoretical aspects" in "Inelastic Particle-Surface Collisions", edited by E. Taglauer and W. Heiland, Springer-Verlag, Berlin, p. 2-37.

Smrcka L. (1970) "Energy band structure of aluminium by the augmented plane wave method" Czech. J. Phys. **B20**, 291-300.

Sternglass E.J. (1957) "Theory of secondary electron emission by high-speed ions" Phys. Rev. **108**, 1-12.

Stolz H. (1959) "Zur Theorie der Sekundärelektronenemission von Metallen. Der Transportprozess" Ann. Phys. **[7] 3**, 197-210.

Streitwolf H.W. (1959) "Zur Theorie der Sekundärelektronenemission von Metallen. Der Anregungsprozess" Ann. Phys. **[7]3**, 183-196.

Svensson B., Holmen G. Buren A. (1981) "Angular dependence of the ion-induced secondary-electron yield from solids" Phys. Rev. **B24**, 3749-3755.

Svensson B., Holmen G. (1982) "Electron emission from aluminium and copper under molecular-hydrogen-ion bombardment" Phys. Rev. **B25**, 3056-3062.

Tabata T., Ito R., Itakawa Y., Itoh N., Morita K. (1983), "Backscattering coefficients of H, D and He ions from solids" At. Data and Nucl. Data Tables **28**, 493-530.

Thomas S., Pattinson E.B. (1970) "Range of electrons and contribution of back-scattered electrons in secondary production in aluminium" J. Phys. D: Appl. Phys. **3**, 349-357.

Tung C.J., Ritchie R.H. (1977) "Electron slowing-down spectra in aluminium metal", Phys. Rev. **B16**, 4302-4313.

Valkealathi S., Nieminen R.M. (1983) "Monte-Carlo calculations of keV electron and positron slowing down in solids", Appl. Phys. **A32**, 95-106.

Williams M.M.R. (1966) "The slowing down and thermalization of neutrons" North-Holland Publishing Company, Amsterdam.

Wolff P.A. (1954) "Theory of secondary electron cascade in metals" Phys. Rev. **95**, 56-66.

#### Discussion with reviewers

R. Bindi : A source function including the contribution of the backscattered electrons and the secondary electron transport gives an isotropic distribution for secondary internal electrons.

Is the validity of the  $P_1$  approximation a consequence of this result?

Authors : Taking the contribution of the backscattered electrons to the source function into account leads to an almost isotropic internal electron source. This justifies partly the  $P_1$  approximation. Moreover, in the secondary electron transport, the importance of the elastic scattering and the slowing down contribute to the isotropy of the internal electron flux. These are the basic supports of the  $P_1$  approximation.

R. Bindi : For the partial yield  $\delta_0$ , you find that 50% of outgoing electrons result from decay of the plasmons and the other 50% from individual excitations. We obtain similar results with our model only if the primary dispersion is taken into account in the source function. Without primary dispersion our model gives the partial yield  $\delta_0$  (Bindi et al., 1980c) and in this case, we find that most electrons are created by plasmon decay according to Chung and Everhart (1977) and Rösler and Brauer (1981b). Could you comment on this discrepancy of the results?

Authors : This discrepancy is probably due to the differences between the assumptions of all authors for the electron interactions in the medium.

You have used Streitwolf's expression (1959) for the binary encounters and Chung and Everhart's formula (1977) for plasmon excitations. Chung and Everhart (1977) don't take the electron multiplication into account in their calculations and the assumptions of Rösler and Brauer (1981a) for plasmon creation and decay are very different from ours. In a much more recent paper, Rösler and Brauer (1988) show that, using dynamical RPA instead of Thomas-Fermi screening, more electrons come from binary collisions than from plasmon decay. The influence of the choice of cross sections is clear and a study of this influence has never been done extensively and could provide a lot of information about electron interactions in solids.

R. Bindi : What parametric studies do you intend to develop?

Authors : We plan to study the influence of the choice of the interaction process of electrons in the medium.

Ganachaud has calculated in his thesis (1977) the influence of the internal ionizations on the electron yield. We plan to extend his work to the influence of the elastic cross section, to the influence of the choice of the dielectric function on the secondary emission properties.

R. Bindi : Could you briefly comment on the advantage of the time dependence?

Authors : Gay and Berry (1979) have for the first time emphasized the importance of secondary emission in beam-foil experiments. It appears that forward emitted electrons could influence the

electronic excitation state of the atoms emerging from thin targets. In order to compute this influence, we need information about the time distribution of outgoing electrons. Calculations are in progress in order to have an idea of the real importance of SEE in such experimental conditions.

P. Rez : I think it ought to be made clear to the reader that the primary electron energies considered in this paper are well below the energies used in the average scanning electron microscopy except in certain low voltage applications. As the authors correctly point out at the low primary energies considered in this paper one should take account of the transport properties of the primary electrons as well as the secondary electrons.

Authors : The primary energies considered in this paper are 0.1-2 keV for incident electrons. It is clear that, for our calculations, the primary electron transport cannot be neglected if we want to adequately reproduce the SEE characteristics.

P. Rez : What evidence is there that  $\phi_c$  is small? I would expect it to be of the same order of magnitude as  $\phi(0, E, \mu)$  to match the boundary conditions.

Authors : Looking at Eq. (18), it is seen that  $\phi_c$  is of the order of magnitude of the infinite medium slowing down solution in the escape cone but it is less outside it. Due to the low energies of outgoing electrons, the escape cone is very narrow for most of them. That is the reason why we use an approximation for  $\phi_c$ . We cannot neglect it but we calculate it approximately because its contribution to the yield is less than the one of  $\phi_0$ . The calculation (with a Monte Carlo code or with a  $S_N$ -multigroup code) of  $\phi(x, E, \mu)$  and the comparison to  $\phi_0(E, \mu)$  is the only way to know the validity of this assumption. Up to now, all comparisons of our model with other calculations seem to demonstrate that this assumption is a correct assumption.

P. Rez : I know that surface plasmons are difficult to incorporate into the theory but I don't think you can dismiss their contribution to electron yield. I would have thought that they would be quite important as low energy primary beams and secondary electrons spend a lot of time in the near surface region.

Authors : Surface plasmons are indeed very difficult to incorporate in transport models. Ganachaud (1977) has incorporated surface plasmons in his Monte Carlo code. Using the code of Ganachaud, we have tried to estimate the influence of surface plasmons on the outgoing electron yield. It appears that the yield is not much modified by the surface zone. We think that the most important influence of surface plasmons is that they are probably responsible for the shoulder at 6 eV in the experimental energy spectrum of outgoing electrons for polycrystalline Al targets.

P. Rez : Both the "improved age-diffusion" model and the transport-albedo model (at least as applied in this paper) assume that the electron

distribution is isotropic (or nearly isotropic). How good is this assumption? The agreement between calculated and experimental energy distributions and the fact that the outgoing angular distribution is a cosine law for electron generated secondaries give support to this view. On the other hand, the forward to backward yield ratio in ion scattering would tend to suggest that something has been neglected. (Though this is partly contradicted by the fact that the calculations appear to have converged by  $l=3$ ). Do you think that a useful step would be to compare angular distributions of secondaries generated by both electron and ion impact with the theory?

Authors : It appears in our calculations that the forward to backward yield ratio is mostly influenced by the  $l=0$  and  $l=1$  terms in the angular development of the flux. Both the  $P_1$  approximation and the transport-albedo model incorporate these terms. It is not evident that the angular distribution provides much information about the internal electron distribution due to the narrowness of the escape cone. Hence, we don't think that the comparison of angular distributions for electron and ion induced emissions can bring much information.

P. Rez : All transport theories neglect the "diffraction" of electron waves. Although it is likely that "diffraction" effects will only change the details of angular distributions and not the total yield, do the authors think that channeling of the incident particle beam (either electrons or ions) could have significant effects on secondary yield?

Authors : It is probable that, in the case of experiments with single crystals, the yield can be reduced by channeling of incident particles. In Auger electron emission (Bishop et al. (1984)), the influence of channeling is important but we don't know if there is some experimental evidence of this effect in SEE.

W. Brauer : What are the explicit expressions of the interaction cross sections used in the calculations of the theoretical yield curves? Is the dynamical screening especially included and what influence is there with respect to the static approximation in the dielectric function?

Authors : We have not incorporated the explicit expressions of the interaction cross sections used in our calculations in the text because this is not the original part of our work. We have used for all our calculations of inelastic interactions the Lindhard's dielectric function. Hence, the dynamical screening is included. Rösler and Brauer (1988) have recently determined the influence of the dynamical screening with respect to the static approximation for electron-electron interactions and concluded to an enhancement of these scattering rates when dynamical screening is included.

W. Brauer : Is the good agreement between experimental and theoretical yield curves a hint for the assumed neglect of excitation of electrons from 2p-core states in the source function?

Authors : No, we intend to incorporate internal ionizations in our calculations. In the energy

range that we have considered for incident electrons, it seems that this contribution is small. For incident ions however, the underestimation of our calculated electron yield over 100 keV for incident  $H^+$  ions seems to emphasize the importance of internal ionizations in this case.

J. Schou : The spatial distribution of the internal source resulting from electron bombardment is based on the range approximation by Kanaya and Kawakatsu (1972). The exponent 4/3 in their expression is much lower than exponents from recent calculations, e.g. by Valkealathi and Nieminen (1983). The value of the exponent is rather about 1.5. Another possibility, that might be tempting is to apply the expression for the spatial energy distribution from Everhart and Hoff (1971) as the source for the internal secondaries. In this way the experimentally determined distribution becomes utilized and the yield induced by the backscattered primaries is automatically included in the secondary electron yield. Everhart and Hoff's expression is a fair approximation for aluminium for primary energies not too far below 5 keV. Would the authors comment on the consequences of these two modifications of the internal electron source?

Authors : We have used other expressions of the range-energy relationship and our results have not been modified in an important way. We have also used a source such as the spatial energy deposition of Everhart and Hoff and obtained rather good results for the outgoing electron yield. Recently, we have incorporated a source resulting from Monte Carlo calculations in the "improved age-diffusion" model and obtained very good results. We have, in fact, preferred to use a source resulting from such a calculation because in this case we have a completely coherent calculation where both the primary and secondary electron interactions are described in the same way.

J. Schou : The calculations in the present work have been performed almost only for the nearly-free-electron metal aluminium. How are the prospects for extending the model to other nearly-free-electron metals and to noble metals and copper?

Authors : There is no objection against the extension of our calculations to other materials. The whole problem is the choice of cross sections for electrons in other materials. The use of semi-empirical cross sections as in Ganachaud's thesis is probably a good solution but more work has still to be done for the extension of our calculations to other materials.

J. Schou : In section 4.1.4 the authors discuss the time distribution of the secondaries as well as the origin of the secondaries, i.e. direct electron-electron excitation or plasmon decay. Is it possible with the frame of the authors' model to indicate a typical time scale for the emission of an electron via plasmon decay, and does the improved age-diffusion model allow the authors to predict any features of the time distribution of

the emitted electrons that are produced by plasmon decay?

Authors : In our calculations, we have considered that plasmon decay instantaneously. The incorporation of a decay time for plasmons requires a little modification of the age-diffusion model. Monte Carlo calculations are in course to estimate the influence of a plasmon decay time on the time distribution of outgoing electrons, but normally, this is also possible with the "improved age-diffusion" model. The typical time scale should be of the order of 1-10 fs.

M. Cailler : It should be very interesting to proceed to a detailed comparison between the results obtained :

- by a description following the techniques developed by Dubus.
- by a description following the techniques developed by Lantéri et al.
- by different Monte Carlo models
- and experimentally

This comparison will bring informations about the validity of each of the theoretical descriptions.

Authors : Your remark is excellent. We think that this comparison should be made in two steps.

1. A detailed comparison of all theoretical calculations with the same set of interaction cross sections
2. When the first step is done, compare the results obtained theoretically with different assumptions for the cross sections to experiments.

In this way, the problems due to the transport description and to the set of interaction cross sections will be clearly separate.

M. Cailler : Information on the accuracy loss arising from the substitution of approximate kernels to cross sections will be helpful.

Authors : We intend to obtain this information by comparing the results obtained in the "infinite medium slowing down" model with the real kernels and the approximate kernels in order to evaluate the influence of this approximation.